Apparatus for dielectric relaxation measurements under high pressure and temperature

Yusuke Hiejima[†] and Makoto Yao[*]

Department of Physics, Graduate School of Science, Kyoto University, Kyoto 600-8502, Japan
[*]E-mail: yao@scphys.kyoto-u.ac.jp

The apparatus and the method of analysis for dielectric relaxation measurements at high temperature and pressure are presented. The microwave spectroscopy developed by our group can be applied for various fluids under extreme conditions. The static permittivity $\varepsilon(0)$ and the Debye-type dielectric relaxation time τ_D of water are obtained in a wide range of temperature and pressure up to the supercritical region.

1. Introduction

Dielectric relaxation is a good probe for rotational dynamics in liquids and solutions. Under ambient conditions, dielectric spectroscopy covers a wide range of frequency from 10^{-6} to 10^{12} Hz [1]. In the microwave region, the time-domain reflectometry (TDR) [2] and the reflection measurements in the frequency domain [3] have been commonly employed. Although the conventional reflection measurements give the complex permittivity $\varepsilon(\omega)$ of the sample precisely in a wide frequency range of several decades, a series of calibration measurements is required.

Our group developed a microwave spectroscopy [4], in which the transmission spectra are used for deducing the dielectric relaxation time. This technique has an advantage of no requirement for calibration procedures at each measurement, though a functional form of $\varepsilon(\omega)$ should be assumed for deducing the dielectric relaxation time. By utilizing the technique we measured dielectric relaxation of water [4], heavy water [5], methanol [6], ethanol and 1-propanol [7] up to the supercritical state. From these measurements the static permittivity $\varepsilon(0)$ and the dielectric relaxation time τ_D were obtained in a wide range of temperature and pressure including the supercritical states. By utilizing the results we interpreted the relaxation processes in water [5] and lower alcohols [6,7] in the whole fluid phase from the gaseous state to the supercooled liquid state.

In this paper, the apparatus and the method of analysis for our microwave spectroscopy is presented. The mathematical basis for the time-domain analysis is described in detail.

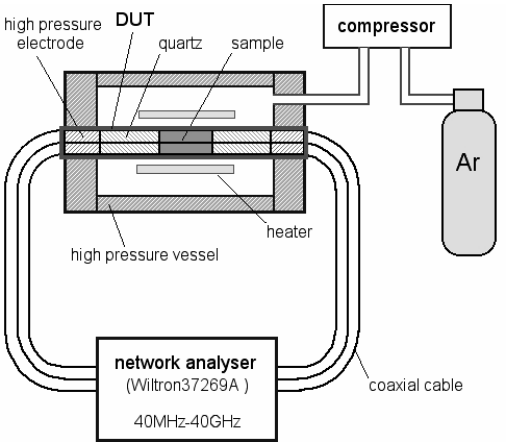

Fig.1. Schematic picture of the apparatus for dielectric relaxation measurements at high temperatures and pressures.

2. Experimental

2.1. Apparatus The apparatus for dielectric relaxation of various fluids up to 200 MPa and 2000 K is schematically shown in Fig. 1. The sample cell had a shape of a coaxial line, and it was composed of platinum outer and inner conductors and quartz glass insulating tubes. In the middle part of the cell, where the quartz tubes were absent, the sample was introduced as the insulating material. The sample cell was placed in a high pressure vessel which was internally heated and pressurized by Argon gas. Each end of the high pressure vessel was closed by a high pressure plug which had a high pressure electrode for introducing the microwave from the outside. Typical experimental

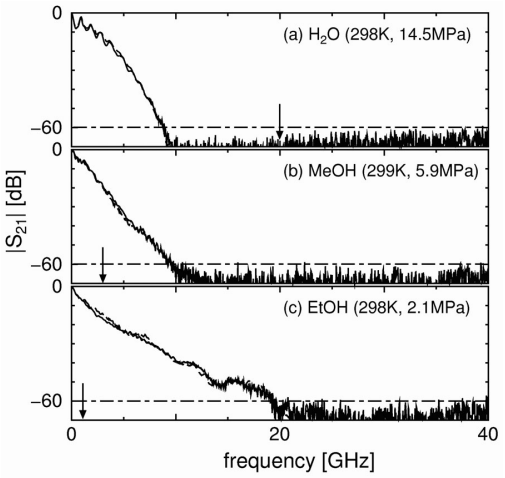

Fig.2. Transmission spectra in the frequency domain for (a) water, (b) methanol and (c) ethanol.

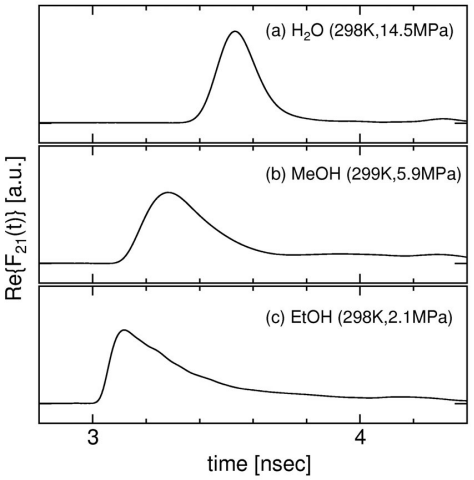

Fig.3. Transmission signals in the time domain for (a) water, (b) methanol and (c) ethanol.

errors in temperature and pressure were less than ±3 K and ±0.2 MPa, respectively.

A vector network analyzer (Wiltron 37269A) was used as both the generator and the receiver of microwaves in the frequency range from 40 MHz to 40 GHz. The device under test (DUT) was an assembly of the sample cell and two high-pressure electrodes. The reflection and transmission spectra were obtained in a form of S matrix (scattering matrix) [8]. The S matrix consists of four S parameters, each of which represents either the complex reflection rate (S_{11}, S_{22}) or the complex transmission rate (S_{12}, S_{21}). The uncertainties in the magnitude and the phase of the microwave transmission rate were 0.1 dB and 1°, those of the reflection rate were 0.3 dB and 2°, respectively.

In Fig. 2, typical transmission spectra are shown by the solid lines. The lower limit of the transmission measurements, namely -60 dB, is denoted by the dash-dotted line. The shape of the transmission spectra are understood by the S matrix for the sample part [9].

$$\log\left|S_{21}^{\text{Sample}}(\omega)\right| \sim -\omega\sqrt{|\varepsilon(\omega)| - \text{Re}\{\varepsilon(\omega)\}}\,, \quad (1)$$

where ε(ω) is the complex permittivity of the sample. The transmission rate is zero at ω=0, and it decreases with increasing ω. Near the dielectric loss band [10], which is indicated by the arrows in Fig. 2, a minimum of the slope is observed for methanol and ethanol.

2.2. Frequency-domain analysis The Debye-type relaxation time τ_D was deduced as follows. The DUT was expressed as cascade connections of the S matrices of two high pressure electrodes (S^{E1} and S^{E2}), two quartz parts (S^{Q1} and S^{Q2}) and the sample part (S^{Sample}).

$$S^{\text{DUT}} = S^{\text{E1}} * S^{\text{Q1}} * S^{\text{Sample}} * S^{\text{Q2}} * S^{\text{E2}}\,, \quad (2)$$

where * denotes the cascade product [8]. Except for the sample part, the individual S matrices were measured or calculated in advance. An appropriate relaxation function was used to describe the relaxation processes of the sample. We found that a Debye function reproduced the experimental spectra in a wide temperature and pressure range of water and lower alcohols [4-7], except for ethanol and 1-propanol near room temperature [7].

$$\varepsilon(\omega) = \varepsilon_\infty + \frac{\varepsilon(0) - \varepsilon_\infty}{1 + i\omega\tau_D}\,. \quad (3)$$

Here the static permittivity ε(0) was obtained from the time-domain signals as described in Section 2.3. The high-frequency permittivity ε_∞ was equated with the square of the refractive index, n^2, which was estimated by the Lorenz-Lorentz equation,

$$\frac{n^2 - 1}{n^2 + 2} = \frac{4\pi\rho\alpha}{3}\,, \quad (4)$$

where the polarizability volume α is 1.45×10^{-24} cm^3 for water [11]. The Debye-type dielectric relaxation time τ_D was determined as such a value that the residual function is minimized.

$$R = \sum_{k=1}^{N} \left\{ \log\left|S_{21}^{\mathrm{calc}}(\omega_k)\right| - \log\left|S_{21}^{\mathrm{exptl}}(\omega_k)\right| \right\}^2, \qquad (5)$$

where $S_{21}^{\mathrm{exptl}}(\omega_k)$ is the experimental transmission rate at the frequency of ω_k, and $S_{21}^{\mathrm{calc}}(\omega_k)$ is that calculated by the model for the DUT. The summation in Eq. (4) was taken over the frequencies at which $|S_{21}^{\mathrm{exptl}}(\omega_k)|$ was larger than the lower limit of transmission measurements.

2.3. Time-domain analysis The impulse response is obtained by the Fourier transform of the components of the S matrix.

$$F_{ij}(t) = \frac{1}{2\pi}\int S_{ij}(\omega) e^{i\omega t} dt \qquad (6)$$

In Fig. 3, the transmission signals in the time domain, which are obtained by the Fourier transform of the transmission spectra shown in Fig. 2, are shown.

The analysis in the time domain is mathematically based on the cumulant expansion.

$$\ln\left(\frac{S_{ij}(\omega)}{S_{ij}(0)}\right) = \sum_{n=1}^{\infty} \frac{\lambda_n^{(ij)}}{n!}(-i\omega)^n \qquad (7)$$

where $\lambda_n^{(ij)}$ is the n-th cumulant. The cumulants are related to the moments [12],

$$\lambda_1^{(ij)} = \left\langle t_{ij} \right\rangle,\ \lambda_2^{(ij)} = \left\langle \left(t_{ij} - \left\langle t_{ij} \right\rangle\right)^2 \right\rangle,\ \lambda_3^{(ij)} = \left\langle \left(t_{ij} - \left\langle t_{ij} \right\rangle\right)^3 \right\rangle, \cdots \qquad (8)$$

The moments are calculated from the time-domain signals F_{ij}(t),

$$\left\langle t_{ij}^n \right\rangle = \frac{\int t^n F_{ij}(t) dt}{\int F_{ij}(t) dt}. \qquad (9)$$

On the other hand, from Eq. (4), the cumulants are written by $S_{ij}(\omega)$,

$$\lambda_n^{(ij)} = \frac{\partial^n}{\partial(-i\omega)^n} \ln\left(\frac{S_{ij}(\omega)}{S_{ij}(0)}\right)\Bigg|_{\omega=0}. \qquad (10)$$

Since $S_{ij}(\omega)$ is a function of the permittivity $\varepsilon(\omega)$ of the sample, the relation between the time-domain signals and the complex permittivity can be deduced by combining Eqs. (8)-(10).

For further calculation, we introduce quantities,

$$\delta\lambda_n \equiv \lambda_n^{(21)} - \frac{\lambda_n^{(11)} + \lambda_n^{(22)}}{2}. \qquad (11)$$

As deduced in Appendices A and B, $\delta\lambda_n$ are described by the coefficients of the complex permittivity $\varepsilon(\omega)$ expanded about ω=0. For n=1, without any assumption for the functional form of $\varepsilon(\omega)$, Eqs. (8), (11) and (A.5) give

$$\left\langle t_{21} \right\rangle - \frac{\left\langle t_{11} \right\rangle + \left\langle t_{22} \right\rangle}{2} = \frac{l_S}{c}\sqrt{\varepsilon(0)}, \qquad (12)$$

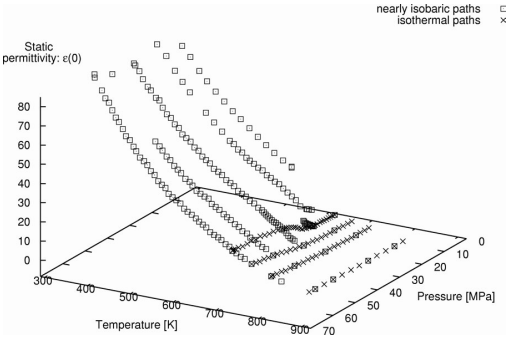

Fig.4. Temperature and pressure dependence of the static permittivity $\varepsilon(0)$ for water along the isothermal paths (crosses) and the nearly isobaric paths (circles).

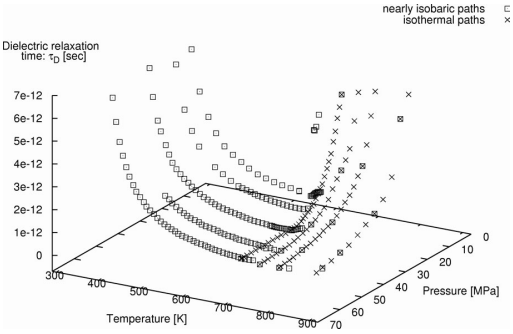

Fig.5. Temperature and pressure dependence of the dielectric relaxation time τ_D for water along the isothermal paths (crosses) and the nearly isobaric paths (circles).

where l_S is the sample thickness (=20 mm) and c is the velocity of light in a vacuum. Eq. (12) directly gives the static permittivity $\varepsilon(0)$ from the time-domain signals.

For n=2, a functional form of $\varepsilon(\omega)$ should be assumed. If a Debye function is assumed for $\varepsilon(\omega)$, from Eqs. (8), (11) and (A.5), the Debye-type relaxation time τ_D are approximately described by

$$\left\langle \left(t_{21} - \left\langle t_{21} \right\rangle\right)^2 \right\rangle \sim \frac{l_S}{c}\frac{\varepsilon(0) - \varepsilon_\infty}{\sqrt{\varepsilon(0)}}\tau_D. \qquad (13)$$

Here $\delta\lambda_2 \sim \lambda_2^{(21)}$ for ambient water and alcohols [9]. As shown in Fig. 3, the position of the transmission signal shifts to shorter time, and the peak becomes broader with increasing the molecular weight. These features are explained by Eqs. (12) and (13), because the static permittivity decreases and the dielectric relaxation time increases in accordance

with the increase of molecular weight for ambient water and alcohols [10].

3. Results and Discussion

3.1. Static permittivity In Fig. 4, the static permittivity ε(0) calculated by Eq. (12) is plotted as a function of temperature and pressure for water from vapor to liquid state. Near room temperature, ε(0) has a large value of 80, and it decreases with density approaching unity in the dilute limit. The values of ε(0) are in very good agreement with a density-expansion formula suggested by Uematsu and Franck [13].

3.2. Dielectric relaxation time The Debye-type dielectric relaxation time τ_D deduced by the frequency-domain analysis in Section 2.2. As shown in Fig. 2, the calculated spectra (dashed lines) well reproduce the experimental spectra (solid lines). Although only the amplitude of the transmission spectrum is utilized in the fitting procedure, the amplitude and the phase of the reflection spectrum, as well as those of the transmission spectrum, are well reproduced by the model in the frequency range up to 40 GHz. In Fig. 5, the resultant τ_D is plotted as a function of temperature and pressure for water. While τ_D in the liquid state rapidly decreases with increasing temperature, it increases with decreasing density in the gaseous state. These temperature and density dependence, which is also observed for lower alcohols [6,7], of τ_D is explained by the binary collision and the life time of hydrogen bond in the whole fluid phase of water [5] and lower alcohols [6,7].

4. Conclusions

The apparatus and the method of analysis for dielectric relaxation measurements at high temperatures and pressures were described. The static permittivity ε(0) was estimated from the time-domain signals, which were the Fourier transform of the components of the S matrix from experiments. The time-domain analysis was mathematically based on the cumulant expansion. The Debye-type dielectric relaxation time τ_D was deduced by the frequency-domain analysis, where τ_D was selected such that the experimental transmission spectrum was reproduced by the calculated one. The static permittivity ε(0) and the dielectric relaxation time τ_D was successfully obtained for water in a wide range of the fluid phase including the supercritical state.

Acknowledgements
This work is partially supported by a Grant-in-Aid for the 21st Century COE. "Center for Diversity and Universality in Physics" in Kyoto University.

Appendix A

In the time-domain analysis, only the direct reflection signals at the quartz/sample interface and the direct transmission signal can be easily distinguished, because the quartz parts are sufficiently long (l_1=65 mm and l_2=59 mm). In such a case, the S matrix without multiple reflections, which is deduced in Appendix B, should be considered for the time-domain analysis.

$$\begin{pmatrix} \tanh(x)\exp[-2\gamma_Q l_1] & \cosh^{-2}(x)\exp[-\gamma_S l_S-\gamma_Q l_1-\gamma_Q l_2] \\ \cosh^{-2}(x)\exp[-\gamma_S l_S-\gamma_Q l_1-\gamma_Q l_2] & \tanh(x)\exp[-2\gamma_Q l_2] \end{pmatrix}. \quad \text{(A1)}$$

Here the propagation constants γ_S for the sample part and γ_Q for the quartz part are given by [13],

$$\gamma_S = \frac{i\omega}{c}\sqrt{\varepsilon(\omega)}, \quad \gamma_Q = \frac{i\omega}{c}\sqrt{\varepsilon_Q} \quad \text{(A2)}$$

and

$$x = -\frac{1}{4}\ln\left(\frac{\varepsilon(\omega)}{\varepsilon_Q}\right). \quad \text{(A3)}$$

By combining Eqs. (A1)-(A3), $\delta\lambda_n$ defined by Eq. (11) is written as

$$\delta\lambda_n = \frac{\partial^n}{\partial(-i\omega)^n}\left[-\gamma_S l_S - \ln\{\cosh(x)\sinh(x)\}\right]\Big|_{\omega=0}. \quad \text{(A4)}$$

In the present study, the second term in the right hand side of Eq. (A4) is negligible except for $\varepsilon(0)\approx\varepsilon_Q$ [14]. Then, $\delta\lambda_n$ is expressed by

$$\delta\lambda_n = -\frac{il_S}{c}\frac{\partial^n}{\partial(-i\omega)^n}\left[\omega\sqrt{\varepsilon(\omega)}\right]\Big|_{\omega=0}. \quad \text{(A5)}$$

Appendix B

The expression of (A1) is deduced as follows. In the time-domain analysis, where only the direct transmission wave through the sample cell and the direct reflection wave at the interface between the quartz part and the sample part are considered, the S matrix is represented by a cascade connection of five S matrices, that is, three matrices for the transmission lines and two matrices for the interfaces [14].

$$S^T(\gamma_Q,l_1)*S^I(Z_Q,Z_S)*S^T(\gamma_S,l_S)*S^I(Z_S,Z_Q)*S^T(\gamma_Q,l_2) \quad \text{(B1)}$$

Here the cascade product of S^A and S^B is defined by [8]

$$S^A * S^B = \begin{pmatrix} S_{11}^A + \dfrac{S_{12}^A S_{21}^A S_{11}^B}{1-S_{22}^A S_{11}^B} & \dfrac{S_{12}^A S_{12}^B}{1-S_{22}^A S_{11}^B} \\ \dfrac{S_{21}^A S_{21}^B}{1-S_{22}^A S_{11}^B} & S_{22}^B + \dfrac{S_{22}^A S_{12}^B S_{21}^B}{1-S_{22}^A S_{11}^B} \end{pmatrix} \quad \text{(B2)}$$

The S matrix for a transmission line, $S^T(\gamma,l)$, with the propagation constant γ and the length l is [14]

$$S^T(\gamma,l) = \begin{pmatrix} 0 & \exp[-\gamma l] \\ \exp[-\gamma l] & 0 \end{pmatrix} \quad \text{(B3)}$$

The S matrix for an interface between two circuits, $S^I(Z_1,Z_2)$, with the characteristic impedance Z_1 and Z_2 is [8]

$$S^I(Z_1,Z_2) = \begin{pmatrix} \dfrac{Z_2-Z_1}{Z_2+Z_1} & \dfrac{2Z_1}{Z_1+Z_2}\dfrac{|Z_2|}{|Z_1|}\sqrt{\dfrac{\mathrm{Re}(Z_1)}{\mathrm{Re}(Z_2)}} \\ \dfrac{2Z_2}{Z_2+Z_1}\dfrac{|Z_1|}{|Z_2|}\sqrt{\dfrac{\mathrm{Re}(Z_2)}{\mathrm{Re}(Z_1)}} & \dfrac{Z_1-Z_2}{Z_1+Z_2} \end{pmatrix} \quad \text{(B4)}$$

The matrix elements of $S^I(Z_1,Z_2)$ can be reduced to simpler forms,

$$S_{11}^I = -S_{22}^I = \tanh(X), \quad S_{12}^I S_{21}^I = \cosh^{-2}(X), \quad \text{(B5)}$$

if we put

$$X = \frac{1}{2}\ln\left(\frac{Z_2}{Z_1}\right). \quad \text{(B.6)}$$

For a coaxial line, in which the permittivity of the insulating material is $\varepsilon(\omega)$, the characteristic impedance $Z(\omega)$ is described as [14]

$$Z(\omega) = \frac{1}{2\pi}\sqrt{\frac{\mu_0}{\varepsilon_0\varepsilon(\omega)}}\log\left(\frac{R_{out}}{R_{in}}\right). \quad \text{(B7)}$$

Here μ_0 and ε_0 are the permeability and permittivity in a vacuum, R_{out} is the inner diameter of the outer conductor, and R_{out} is the outer diameter of the inner conductor. Since R_{out} and R_{in} are constant for the sample cell, X in Eq. (B6) is simply described by the permittivity. For $S^I(Z_Q,Z_S)$, X is replaced by x given by Eq. (A3). Then, the S matrix of (B1) is calculated to be

$$\begin{pmatrix} \dfrac{\tanh(x)\exp[-2\gamma_Q l_1](1-\exp[-2\gamma_S l_S])}{1-\tanh^2(x)\exp[-2\gamma_S l_S]} & \dfrac{\cosh^{-2}(x)\exp[-\gamma_Q l_1-\gamma_Q l_2-\gamma_S l_S]}{1-\tanh^2(x)\exp[-2\gamma_S l_S]} \\ \dfrac{\cosh^{-2}(x)\exp[-\gamma_Q l_1-\gamma_Q l_2-\gamma_S l_S]}{1-\tanh^2(x)\exp[-2\gamma_S l_S]} & \dfrac{\tanh(x)\exp[-2\gamma_Q l_2](1-\exp[-2\gamma_S l_S])}{1-\tanh^2(x)\exp[-2\gamma_S l_S]} \end{pmatrix} \quad \text{(B.8)}$$

From simple argument, one may see that the neglect of the multiple reflection is equivalent to removal of the term $\exp[-2\gamma_S l_S]$. Thus, (A1) is obtained.

References and Notes

[1] F. Kremer, *J. Non-Cryst. Solids*, **305**, 1 (2002).
[2] H. F-. Feldegg, *J. Phys. Chem.*, **73**, 616 (1969).
[3] Y. Z. Wei and S. Sridhar, *Rev. Sci. Instrum.*, **60**, 3041 (1989).
[4] K. Okada, Y. Imashuku, and M. Yao, *J. Chem. Phys.*, **107**, 9302 (1997).
[5] K. Okada, M. Yao, Y. Hiejima, H. Kohno, and Y. Kajihara, *J. Chem. Phys.*, **110**, 3026 (1999).
[6] Y. Hiejima, Y. Kajihara, H. Kohno, and M. Yao, *J. Phys Condens. Matter.*, **13**, 10307 (2001).
[7] Y. Hiejima and M. Yao, *J. Chem. Phys.*, **119**, 7931 (2003).
[8] R. B. Marks and D. F. Williams, *J. Res. Nat. Inst. Stand. Tech.*, **97**, 533 (1992).
[9] Y. Hiejima, Thesis, Kyoto University (2004).
[10] J. Barthel, K. Bachhuber, R. Buchner, and H. Hetzenauer, *Chem. Phys. Lett.*, **165**, 369 (1990).
[11] *CRC Handbook of Chemistry and Physics,* 68th. ed. (Chemical Rubber Co., Boca Raton, FL, 1987).
[12] H. Cramér, *Mathematical Methods of Statistics*, (Princeton University Press, 1946).
[13] M. Uematsu and E. U. Franck, *J. Phys. Chem. Ref. Data*, **9**, 1291 (1980).
[14] M. Sucher and J. Fox, *Handbook of Microwave Measurements*, (Polytechnic Press, Brooklyn, 1963).

† Present Address: Supercritical Fluid Research Center, National Institute of Advanced Industrial Science and Technology (AIST),
4-2-1 Nigatake, Miyagino-ku, Sendai 983-8551, Japan
E-mail: y-hiejima@aist.go.jp